

Reflectance Estimation under Complex Illumination

Du Fei[†] Takahiro Okabe[†] Yoichi Sato[†] Akihiro Sugimoto^{††}

Abstract: In this paper, we propose a method for recovering the albedo of a convex Lambertian object by using multiple images taken with a fixed view point and different poses under complex illumination, provided that the shape and pose of the object are known but the illumination condition is unknown. Our proposed method estimates the albedo of the object based on observations that images of a Lambertian object under varying illumination conditions can be approximately represented by using low-order spherical harmonics. To demonstrate the effectiveness of our method, we conducted a number of experiments by using synthesized images.

1 Introduction

In computer graphics, we generally use an ideal surface, the Lambertian surface, to approximate many kinds of materials without specular reflectance. A Lambertian surface appears to be equally bright from all viewing directions; in other words, it reflects light proportional to the irradiance. So the analysis of this physical system is equal to the analysis of the relationship between irradiance and brightness. For a Lambertian object, the image irradiance is known to be a function of the following three components: the distribution of light sources; the shape of the object; and the albedo, which is a ratio of the incident light re-emitted by the surface. Depending on the relationship among them, we can recover one component or two components from the image.

In this paper, we present a new method to estimate the albedo of a convex, Lambertian object by using multiple images under the same general illumination distribution with fixed viewpoints and different object poses. We assume that the geometry of the object is known, while its illumination condition is unknown. The illumination distribution, which is relatively distant, can include an arbitrary combination of point source, extended source and diffuse light. The convex shape of object ensures that there are no cast shadows and interreflection.

Our work is based on the recent theoretical analysis by Ramamoorthi and Hanrahan[1], who attempted to represent the convolution form of reflection[2] in terms of spherical harmonic function, and showed that the Lambertian reflectance can be approximated by using low order spherical harmonics. (Basri and Jacobs[3] did similar work in face recognition.) According to this theoretical analysis, we can construct approximate equation of Lambertian reflectance in terms of low-order spherical harmonic function. One image of the object can provide many independent equations according to distinct normal directions on the object. If we ro-

tate the object for some number of degrees and obtain a new image, we can get more equations. In these equations only the harmonic coefficients of illumination function and the albedo are unknown, so what we should do is to obtain their solutions from these equations.

Finally, we present some preliminary experiments using synthetic images to illustrate the potential of our proposed method. We use multiple images obtained by rotating a football and a textured cube under global illumination[4]. We show that we can recover the albedo of the Lambertian surface to a high degree of accuracy and the recovered albedo is robust against the errors in geometry, so that our work also can be combined with the algorithm of shape-from-motion(SFM)[5]. SFM enables us to recover the shape of the object first by using the object's images with different poses; then, on the basis of the shape estimation, we can further recover the albedo of the object. We also explain why there are errors in the solution of harmonic coefficients of the illumination function and find that, by using recovered harmonic coefficients, we can obtain a very similar illumination distribution over the hemisphere centered at the camera viewing direction.

The remainder of this paper is organized as follows. In section 2, we introduce some previous work. In Section 3, we describe the spherical harmonic representation of the brightness and further explain the approximation of the brightness for Lambertian surface with low order spherical harmonics. In Section 4, we introduce proposed method to recover the albedo with known object's geometry by using multiple images of that object with different poses. In Section 5, we present experimental results to verify the validation of our proposed method. We also confirm that our method is robust against the errors of geometry through experiment and explain why there are errors in the solutions of the illumination function. Finally, in Section 6, we present our conclusions and give directions for some future work.

[†] Institute of Industrial Science, The University of Tokyo

^{††} National Institute of Informatics

2 Previous Work

There are two representative methods that can recover the albedo: the inverse-rendering method[9, 10]; and the photometric stereo method[6, 7, 8]. The inverse rendering method[2, 9, 10, 11, 12, 13, 14], assuming known geometry, recovers lighting and/or reflectance properties from images of objects. Our proposed method belongs to the inverse rendering field. The photometric stereo method can recover a Lambertian object's shape and albedo by using multiple images of a fixed object scene with variable illumination conditions. In contrast to these methods, Nakashima et al.[15] estimated both geometric and photometric properties of an object from an image sequence of the object in motion.

In the previous work, albedo could be well recovered under a single point source[6, 9, 15]; however, the single point source condition exists only for laboratory conditions and seems impractical for outdoors. So now many researchers are trying to recover albedo under general illumination conditions. There are two representative methods to recover albedo of the object under general illumination [8, 10]. We compare their assumption with our work in Table 1. In the inverse rendering

Table 1: Comparison with previous work

Method	View point	Pose	Illumination
Nishino et al.[10]	variable	fixed	fixed
Basri and Jacobs[8]	fixed	fixed	variable
Proposed	fixed	variable	fixed

field, Nishino et al.[10] were able to recover reflectance properties and general illumination distribution by using images of a fixed object with different viewpoints and same illumination conditions. In the photometric stereo field, Basri and Jacobs[8] proposed a method to recover the albedo and shape of the object under general illumination condition by using images of a fixed object scene with fixed viewpoint and variable illumination conditions.

Our work seems to be more practical than the previous work[6, 7, 9] as our proposed method is suitable for arbitrary general illumination conditions. For the unconstrained lighting, method proposed by Basri and Jacobs[8] requires that each image of the object should be taken under variable general lighting conditions; our method, on the other hand, needs only multiple images taken with different poses under the same general illumination conditions. Thus, it appears that our method is simpler in the image preparation process. Additionally, some methods in photometric stereo[7, 8] encountered the ambiguity question[16] and could only recover the shape and albedo to a linear transfer combination. The method proposed by Nishino et al.[10]

used the information from specular parts to estimate illumination distribution. Their method is not suited for diffuse illumination conditions, while our method is suited for arbitrary illumination conditions.

3 Spherical Harmonic Representation of the Reflectance

3.1 Reflection Equations of Lambertian Surface

We suppose that the illumination is distant from the object. Let lighting direction be (θ_i, ϕ_i) and normal direction is (α, β) by using view direction as reference. We also suppose that the surface is convex, thereby ensuring that there are no cast shadows or interreflections. Accordingly, we know that the irradiance is due only to θ'_i , which is the angle between (θ_i, ϕ_i) and (α, β) . Now the irradiance's equation becomes to:

$$E(\alpha, \beta) = \int_{\Omega} L(\theta_i, \phi_i) A(\theta'_i) d\Omega,$$

where $L(\theta_i, \phi_i)$ is the distant illumination function.

$$A(\theta'_i) = \max(\cos\theta'_i, 0), \quad (1)$$

For Lambertian surface, observed brightness can be related to the irradiance as $I(\alpha, \beta) = \rho E(\alpha, \beta) / \pi$, where ρ between 0 and 1 is the albedo, then we can get the equation of $I(\alpha, \beta)$,

$$I(\alpha, \beta) = \rho' \int_{\Omega} L(\theta_i, \phi_i) A(\theta'_i) d\Omega, \quad \rho' = \frac{\rho}{\pi}. \quad (2)$$

3.2 Spherical Harmonic Representation of Reflectance

Now we want to construct a closed-form description of the observed brightness of the Lambertian surface in terms of spherical harmonic coefficients.

First, we want to give the definition of a spherical harmonic

$$Y_{l,m}(\theta, \phi) = \begin{cases} \sqrt{\frac{(2l+1)(l-m)!}{2\pi(l+m)!}} P_l^m(\cos\theta) \sin(m\phi) & (m = 1, 2, 3, \dots, n) \\ \sqrt{\frac{(2l+1)}{4\pi}} P_l(\cos\theta) & (m = 0) \\ \sqrt{\frac{(2l+1)(l-|m|)!}{2\pi(l+|m|)!}} P_l^{|m|}(\cos\theta) \sin(m\phi) & (m = -1, -2, -3, \dots, -n) \end{cases} \quad (3)$$

where P_l, P_l^m are Legendre polynomial and associated Legendre function; then we can expand the function

$L(\theta_i, \phi_i)$, $A(\theta'_i)$ in terms of spherical harmonics as follows:

$$L(\theta_i, \phi_i) = \sum_{l=0}^{\infty} \sum_{m=-l}^{+l} L_{l,m} Y_{l,m}(\theta_i, \phi_i), \quad (4)$$

$$A(\theta'_i) = \sum_{l=0}^{\infty} A_l Y_{l,0}(\theta'_i). \quad (5)$$

Here, the coefficients L_{lm} and A_l can be computed in the standard way by integrating against the Y_{lm}

$$L_{lm} = \int_{\theta_i=0}^{\pi} \int_{\phi_i=0}^{2\pi} L(\theta_i, \phi_i) Y_{lm}(\theta_i, \phi_i) \sin\theta_i d\theta_i d\phi_i, \quad (6)$$

$$A_l = 2\pi \int_{\theta'_i=0}^{\pi} A(\theta'_i) Y_{l,0}(\theta'_i) \sin\theta'_i d\theta'_i. \quad (7)$$

Substituting equation(4) and (5) into equation(1), we can get the multiplication form of irradiance in the frequency domain [1] by orthonormality of the spherical harmonics

$$E(\alpha, \beta) = \sum_{l=0}^{\infty} \sum_{m=-l}^{+l} \sqrt{\frac{4\pi}{2l+1}} A_l L_{l,m} Y_{l,m}(\alpha, \beta). \quad (8)$$

Among them, the values of A_l can be computed according to the equation(7):

$$A_l = \begin{cases} \sqrt{\pi}/2 & l = 0 \\ \sqrt{\pi}/3 & l = 1 \\ 2\pi \left(\frac{2n+1}{4\pi}\right)^{1/2} \frac{(-1)^{n/2-1}}{(n+2)(n-1)} \\ \times \left[\frac{n!}{2^n (n!/2)^2}\right] & l > 2, \text{even} \\ 0 & l \geq 2, \text{odd} \end{cases} \quad (9)$$

The asymptotic behavior of A_l for large even l is $A_l \sim l^{-2}$ while $A_l = 0$ for odd $l > 1$, so we can omit $A_l (l > 2)$ and estimate irradiance by using only the first three terms. Considering the relation between the observed brightness and irradiance of Lambertian surface, we can get the approximation of $I(\alpha, \beta)$,

$$I(\alpha, \beta) \approx \rho'(\alpha, \beta) \sum_{l=0}^2 \sum_{m=-l}^{+l} \sqrt{\frac{4\pi}{2l+1}} A_l L_{l,m} Y_{l,m}(\alpha, \beta), \quad (10)$$

which is a sum of 9 terms.

Now we want to use the direction of surface's normal (x, y, z) which can be easily obtained to replace the angles α, β , by substituting the following relations:

$\alpha = \cos^{-1} z, \beta = \tan^{-1}(y/x)$. The first nine harmonics then become to

$$\begin{aligned} Y_{0,0} &= \frac{1}{\sqrt{4\pi}} & Y_{1,-1} &= \sqrt{\frac{3}{4\pi}} x \\ Y_{1,0} &= \sqrt{\frac{3}{4\pi}} z & Y_{1,1} &= \sqrt{\frac{3}{4\pi}} y \\ Y_{2,-2} &= \frac{3}{2} \sqrt{\frac{5}{12\pi}} (x^2 - y^2) & Y_{2,-1} &= 3 \sqrt{\frac{5}{12\pi}} xz \\ Y_{2,0} &= \frac{1}{2} \sqrt{\frac{5}{4\pi}} (2z^2 - x^2 - y^2) & Y_{2,1} &= 3 \sqrt{\frac{5}{12\pi}} yz \\ Y_{2,2} &= 3 \sqrt{\frac{5}{12\pi}} xy. \end{aligned} \quad (11)$$

Substituting the first nine harmonics as well as the values of coefficient $A_l (l = 0, 1, 2)$ into the equation (10), we can get the observed brightness expression of the Lambertian surface in terms of the normal direction (x, y, z)

$$\begin{aligned} I(x, y, z) &\approx \rho'(x, y, z) \left[\frac{\sqrt{\pi}}{2} L_{0,0} + \sqrt{\frac{\pi}{3}} L_{1,0} z + \sqrt{\frac{\pi}{3}} L_{1,1} y \right. \\ &+ \sqrt{\frac{\pi}{3}} L_{1,-1} x + \frac{\sqrt{5\pi}}{16} L_{2,0} (2z^2 - x^2 - y^2) \\ &+ \frac{\sqrt{15\pi}}{8} L_{2,1} yz + \frac{\sqrt{15\pi}}{8} L_{2,2} xy \\ &\left. + \frac{\sqrt{15\pi}}{8} L_{2,-1} xz + \frac{\sqrt{15\pi}}{16} L_{2,-2} (x^2 - y^2) \right]. \quad (12) \end{aligned}$$

4 Proposed Method

In this part we begin to explain how to recover the albedo with the known object's geometry and multiple images of the object taken with a fixed viewpoint and different poses.

The equation (12) forms the basis of our proposed method. We have known the normal direction (x, y, z) of each point on the object. The values of $I(x, y, z)$ of all the visible points can be obtained from one image of the object. So in these equations, only $\rho'(x, y, z)$ and $L_{l,m} (l = 0, 1, 2; -l \leq m \leq l)$ are unknowns and what we should do is to obtain their solutions.

Given one image, we can choose n visible points with different normal directions to construct n independent equations. More equations will be provided from multiple images of the object with different poses. The unknowns $\rho'(x, y, z)$ and $L_{l,m}$ are in multiplication form in the equation. So it is impossible to solve for the specific values of $\rho'(x, y, z)$ and $L_{l,m}$. To overcome this difficulty, we can assume that the albedo of some point is equal to 1, and then solve $L_{l,m}$ and relative $\rho'(x, y, z)$ from the equations. Furthermore, because all the equations are approximate equations, we try to get the most approximate solutions of $\rho'(x, y, z)$ and $L_{l,m}$ by solving a set of over-constrained linear equations.

4.1 Solving $L_{l,m}$

Because the unknowns ρ' and $L_{l,m}$ are in multiplication form, we should first remove the unknowns ρ' to get equations only according to $L_{l,m}$. Suppose that $\bar{\rho}(x, y, z) = \rho'(x, y, z)L_{0,0}$ and $\bar{L}_{l,m} = L_{l,m}/L_{0,0}$; then equation (12) will change to

$$I_i^{(j)} \approx \bar{\rho}_i \left(\frac{\sqrt{\pi}}{2} + \sqrt{\frac{\pi}{3}} \bar{L}_{1,0} z_i^{(j)} + \sqrt{\frac{\pi}{3}} \bar{L}_{1,1} y_i^{(j)} + \dots \right),$$

$$(i = 1, 2 \dots n; j = 1, 2 \dots s). \quad (13)$$

Here i means different point and j means different poses of the object. We suppose that a total of n visible points and s variable poses have been chosen.

Now we want to get the ratios of the corresponding points' observed brightness with different pose. Supposing that $I_i^{(j+1)}/I_i^{(j)} = k_i^{(j)}$, we can get $n(s-1)$ equations about $\bar{L}_{l,m}$:

$$-\frac{\sqrt{\pi}}{2}(k_i^{(j)} - 1) \approx \sqrt{\frac{\pi}{3}} \bar{L}_{1,0}(k_i^{(j)} z_i^{(j)} - z_i^{(j+1)})$$

$$+ \sqrt{\frac{\pi}{3}} \bar{L}_{1,1}(k_i^{(j)} y_i^{(j)} - y_i^{(j+1)}) + \dots,$$

$$(i = 1, 2 \dots n; j = 1, 2 \dots s - 1). \quad (14)$$

By now we have removed the unknown $\bar{\rho}_i (i = 1 \dots n)$.

Because all the equations are approximation equations, we obtain the optimal solutions of $\bar{L}_{l,m}$ in the sense of the least square error.

4.2 Recovering the Albedo of Each Visible Point

Then we want to substitute the solution of $\bar{L}_{l,m}$ into the following equation to recover the $\bar{\rho}_i$ of every visible point.

$$\bar{\rho}_i = \frac{I_i}{\frac{\sqrt{\pi}}{2} + \sqrt{\frac{\pi}{3}} \bar{L}_{1,0} z_i + \sqrt{\frac{\pi}{3}} \bar{L}_{1,1} y_i + \dots}, (i = 1 \dots n). \quad (15)$$

Because albedo is a relative value, we should set a standard albedo and get the relative value of albedo $\tilde{\rho}_i$ according to the standard. Supposing that $\tilde{\rho}_1 = 1$, we can get the relative albedo of other points by

$$\tilde{\rho}_i = \bar{\rho}_i / \bar{\rho}_1 = \rho_i / \rho_1 (2 \leq i \leq n). \quad (16)$$

5 Experimental Results

We now describe some preliminary experiments in which we used synthetic images to verify the effectiveness of our method. We used two objects: a football and a textured cube. We placed them under a global illumination and verified that our algorithm could recover the

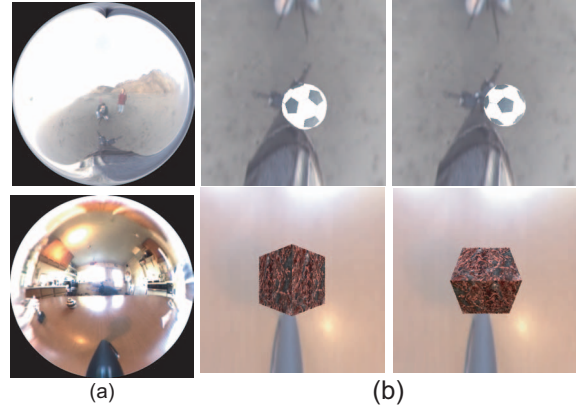


Figure 1: **Synthetic images under general illumination:** (a) Light probe images. (b) Synthetic images under general illumination conditions.

albedo/texture of the surfaces to a high degree of accuracy. At last we will confirm that our method is robust against the errors of geometry, so that our method can be combined with SFM.

5.1 Radiance and Light Probe Image

Radiance Synthetic Imaging System[19] is a highly accurate ray-tracing software system, which can provide simulation results as color images, numerical values and contour plots according to the input files, including the scene geometry, materials, and illumination conditions. We used it to produce the synthetic images used in the experiment.

Light probe image is an omni-directional, high dynamic range image that records the incident illumination conditions at a particular point in space. We can use such images to render a synthetic object into real scenes[4]. Fig.1 (a) shows two examples of the light probe images.

5.2 Recovering Albedo

We used two objects, a football and a textured cube, to verify the validation of our proposed method.

As described in 5.1, we used Radiance and Probe Image to produce the synthetic images under general illumination as Fig.1 (b) shows. The input files included lighting conditions, camera parameters, shape, materials, location and pose of the object. According to the camera parameters, we could get the brightness of arbitrary visible point on the object from the corresponding point on the image. Radiance can provide simulation results as numerical values, so k_i^j , the ratio of some visible point's brightness with different poses, could be

Table 2: **Recovered albedo of football**

	ρ_r		ρ_g		ρ_b	
1	0.100		0.100		0.100	
2	0.901	9.9%	0.909	9.1%	0.920	8.0%
3	0.102	2.0%	0.101	1.0%	0.101	1.0%
4	0.988	1.2%	0.989	1.1%	0.998	1.2%
5	0.973	2.7%	0.974	2.6%	0.982	1.8%
6	0.976	2.4%	0.978	2.2%	0.986	1.4%
7	1.025	2.5%	1.027	2.7%	1.030	3.0%
8	0.102	2.0%	0.102	2.0%	0.102	2.0%
9	0.969	3.1%	0.971	2.9%	0.982	1.8%
10	0.102	2.0%	0.102	2.0%	0.102	2.0%
Ground Truth		1.000	2 4 5 6 7 9			
$(\rho_r = \rho_g = \rho_b)$		0.100	1 3 8 10			

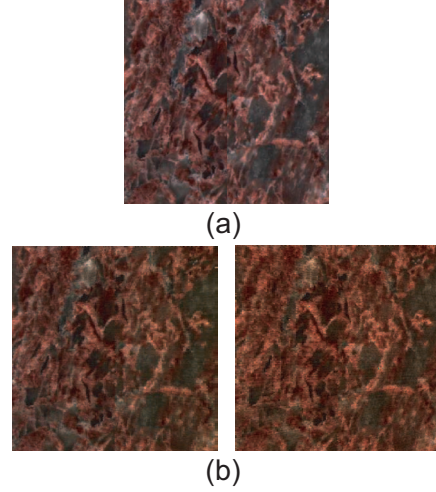


Figure 2: **Recovered texture of the cube:** (a) Original texture. (b) Recovered textures.

Table 3: **Errors of the representative points of cube:**

	ρ_r		ρ_g		ρ_b	
1	1.000		1.000		1.000	
2	1.003	0.3%	1.006	0.6%	0.998	0.2%
Ground truth of point 2 ($\rho_r = \rho_g = \rho_b$)						1.000

obtained easily. By substituting k_i^j and normals' directions x_i^j, y_i^j, z_i^j into the simultaneous equations (14), we could solve the most approximate solutions of $\bar{L}_{l,m}$ in the sense of the least square error. Then we substituted the solutions of $\bar{L}_{l,m}$ into the equations (15) to solve the $\bar{\rho}_i$ and further recovered the relative albedo $\tilde{\rho}_i$, supposing $\tilde{\rho}_1 = 1$.

The result shown in Table 2 illustrates the recovered relative albedo of nine arbitrary points on the football comparing to the point 1. We computed the error by comparing the ground truth. For the textured cube, we only compute the albedo of one representative point on one face and then recovered the texture of the face according to the proportion relation of the brightness. Fig.2 (a) is the original texture of the cube and (b) are recovered texture of two faces of the cube. We also compute the errors of the albedo of the representative points similarly and showed the results in Table 3.

5.3 Errors in $L_{l,m}$

Our proposed method recovers the spherical harmonic coefficients $L_{l,m}$ of the lighting simultaneously, but Table 4 shows that the recovered value of $L_{l,m}$ are not correct. The reason is that the images taken with one camera used to solve the solutions of $L_{l,m}$ do not include the lighting comes from different directions equa-

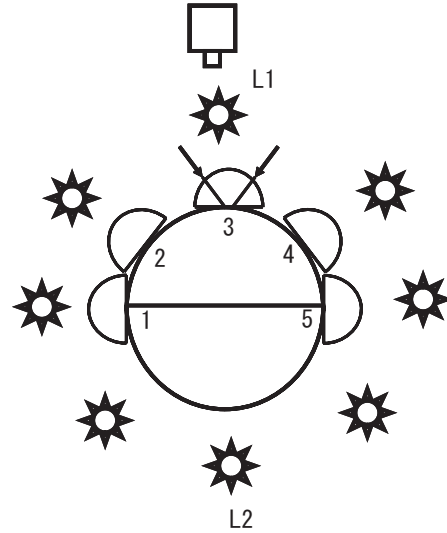


Figure 3: **Analysis of $L_{l,m}$'s Solution**

lly. As Fig.3 shows, with one camera we can only measure the brightness of the points whose normal directions belong to a hemisphere, such as points from 1 to 5. Now think about one extreme situation that when the lighting comes from the same direction of camera as light $L1$, all the visible points will include its information. For the other extreme situation that when the lighting comes from the contrary direction of camera as light $L2$, only the points 1 and 5 which are on the edge of the hemisphere will include its information. So the equations constructed according to these points' brightness are also not equal to lighting comes from different directions. We solved this set of approximated equa-

Table 4: **Recovered** L_{lm} (R:recovered T:ground truth)

$L_{l,m}$	$L_{0,0}$	$L_{1,0}$	$L_{1,1}$	$L_{1,-1}$	$L_{2,0}$	$L_{2,-1}$	$L_{2,1}$	$L_{2,-2}$	$L_{2,2}$
R	1.000	-0.117	-0.295	-0.372	-0.344	0.110	-0.180	-0.166	-0.191
T	1.000	-0.253	0.463	-0.660	-0.047	0.238	-0.124	-0.0003	-0.0001

tions in the sense of the least square error. If there is some error about the solution of light $L1$, because all the equations include its information, the error will be enlarged many times. On the contrary, because only a few equations include the information of light $L2$, the error about it will be neglected. So there are some errors in the solutions of $L_{l,m}$.

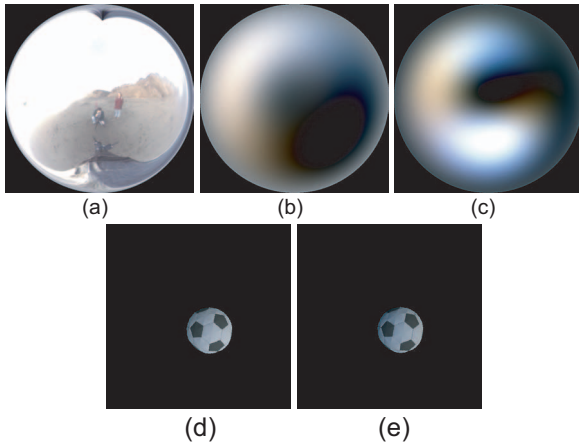


Figure 4: **Recovered illumination distribution:** (a) Original probe image. (b) Low-order simulation of illumination obtained from real $L_{l,m}$. (c) Low-order simulation of illumination obtained from recovered $L_{l,m}$. (d) Synthetic images by using illumination in (b). (e) Synthetic images by using illumination in (c).

Although the recovered values of $L_{l,m}$ are not correct, because the least square error ensures that the solved solutions are the most approximate solutions to satisfy the equations, the errors will not affect the accuracy of the recovered albedo. From the above analysis, we could conjecture that, by using the recovered $L_{l,m}$, we could approximately recover the illumination distribution over the hemisphere centered at the camera viewing direction. Fig.4 verifies our conjecture. Fig.4 (a) is the original probe image of beach, from which we could obtain the lighting intensity $L(\theta_i, \phi_i)$; then substituting the values of $L(\theta_i, \phi_i)$ into the equation(6) we could compute the real values of $L_{l,m}$. After the real and recovered values of $L_{l,m}$ had been obtained, we could get the low-order simulation of illumination distribution according to the equation (4). Fig.4 (b) is the low-order simulation obtained by using real $L_{l,m}$, while Fig.4 (c) is the one obtained by using recovered

$L_{l,m}$. By comparing (b) and (c), we can find out that the illumination of the upper hemispheres, which is centered at the camera viewing direction, are similar to each other. We also used these two low-order simulation of illumination to synthesize images of a football as Fig.4 (d) and (e) which are also very similar to each other.

5.4 Sensitivity Analysis Against Geometrical Errors

In this part, we want to analyze the sensitivity of our proposed method against geometrical errors. We artificially insert errors into the geometry of the object and then observe the relation between errors of recovered albedo and artificial errors of geometry. We choose a total of ten points in the experiment and for each point we let the angle between the directions of new normal and original normal be $(\Delta\theta, \Delta\phi)$, in which $\Delta\theta$ is a random number according to normal distribution and $\Delta\phi$ is a uniform random number from 0^0 to 360^0 . Fig.5 shows the result of two representative points. The abscissa is the standard deviation σ of the distribution of $\Delta\theta$; the ordinate is about the absolute errors of the recovered albedo. For every σ , we performed the experiment 500 times and computed the mean and standard deviation of the errors. From Fig.5 we can find that, although there are some errors in the geometry, we still can recover albedo to a high degree of accuracy.

Because our proposed method is robust against the errors of geometry, we can try to combine proposed method with the SFM method and use only multiple images taken with variable poses of the object to recover the albedo. First, we can estimate the object's shape from multiple images of the object with different poses by using SFM; then, on the basis of the recovered shape of the object, we can further recover the albedo of the object with our proposed method.

6 Conclusion and Future Work

In this paper, we have presented a new method to recover the albedo of a convex, Lambertian object under a general and distant illumination condition. Our algorithm belongs to the inverse rendering field. We recovered the albedo by using a known object's geometry and multiple images taken with a fixed viewpoint and different poses. We have done some preliminary experiments by using synthetic images to show that we can

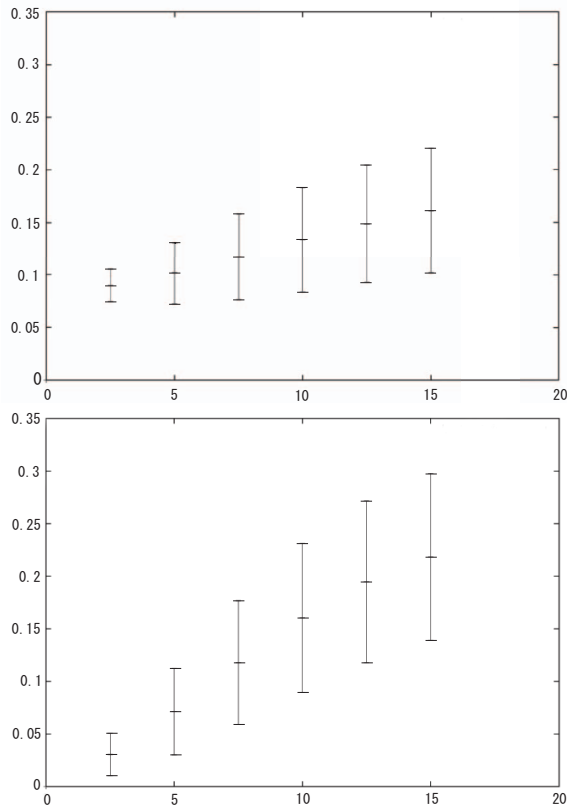


Figure 5: Sensitivity analysis against geometrical errors

recover the albedo to a high degree of accuracy. Unfortunately, because the equations are not equal to lighting coming from different directions, there are some errors in the solution of $L_{l,m}$ obtained in the sense of the least square error, but it will not affect the accuracy of the recovered albedo. We also verified that, by using the recovered $L_{l,m}$, we can get similar lighting distribution over the hemisphere centered at the camera viewing direction.

In the future, we should do experiments under the actual illumination distribution to verify the validity of our proposed algorithm. At the same time, we will combine our proposed method with SFM and recover the albedo of an object using only multiple images taken by varying the pose of the object. We also want to extend our proposed method to make it suitable for more complex reflectance properties beyond the Lambertian model.

Acknowledgements

This research was in part supported by Grant-in-Aid for Scientific Research of the Ministry of Education, Culture, Sports, Science and Technology of Japan (No. 13224051 and No. 14380161.)

References

- [1] R. Ramamoorthi and P. Hanrahan, "On the Relationship between Radiance and Irradiance: Determining the Illumination from Images of a Convex Lambertian Object", *J. Optical Soc. Am. A*, 18(10): 2448–2459, 2001.
- [2] G. Miller, and C. Hoffman, "Illumination and reflection maps: simulated objects in simulated and real environments", In *Proc. ACM SIGGRAPH '84 course notes*, 1984.
- [3] R. Basri and D. Jacobs, "Lambertian Reflectance and Linear Subspaces", In *Proc. IEEE ICCV*, pp.383–390, 2001.
- [4] P. Debevec, "Rendering synthetic objects into real scenes: bridging traditional and image-based graphics with global illumination and high dynamic range photography", In *Proc. ACM SIGGRAPH '98*, pp.189–198, 1998.
- [5] C. Tomasi and T. Kanade, "Shape and motion from image streams under orthography: a factorization method", *Int'l. J. Computer Vision*, 9(2):137–154, 1992.
- [6] R. Woodham, "Photometric method for determining surface orientation from multiple images", *Optical Engineering*, 19(1):139–144, 1980.
- [7] A. Yuille, D. Snow, R. Epstein, and P. Belhumeur, "Determining generative models of objects under varying illumination: shape and albedo from multiple images using SVD and integrability", *Int'l. J. Computer Vision*, 35(3):203–222, 1999.
- [8] R. Basri and D. Jacobs, "Photometric stereo with general, unknown lighting", In *Proc. IEEE CVPR 2001*, 2, pp.374–381, 2001.
- [9] Y. Sato, M. Wheeler, and K. Ikeuchi, "Object shape and reflectance modeling from observation", In *Proc. ACM SIGGRAPH 97*, pp.379–387, 1997.
- [10] K. Nishino, Z. Zhang, and K. Ikeuchi, "Determining reflectance parameters and illumination distribution from sparse set of images for view-dependent image synthesis", In *Proc. IEEE ICCV 2001*, pp.599–606, 2001.
- [11] I. Sato, Y. Sato, and K. Ikeuchi, "Illumination distribution from shadows", In *Proc. IEEE CVPR '99*, pp.306–312, 1999.
- [12] T. Okabe, I. Sato, Y. Sato, K. Ikeuchi, "Estimation of Illumination Distribution from Cast Shadows: Analysis Based on Spherical Harmonics Expansions", In *Proc. MIRU 2002*, vol.1, pp.461–468, 2002. (in Japanese)
- [13] A. Marschner, and D. Greenberg, "Inverse lighting for photography", In *Fifth Color Imaging Conference*, pp.262–265, 1997.
- [14] R. Ramamoorthi and P. Hanrahan, "A signal-processing framework for inverse rendering", In *Proc. ACM SIGGRAPH 2001*, pp.117–128, 2001.
- [15] A. Nakashima, A. Maki, and K. Fukui, "Constructing illumination image basis from object motion", In *Proc. ECCV 2002(LNCS 2352)*, pp. 195–209, 2002.
- [16] P. Belhumeur, D. Kriegman, and A. Yuille, "The bas-relief ambiguity", In *Proc. IEEE CVPR 1997*, pp.1040–1046, 1997.
- [17] B. K. P. Horn, *Robot Vision*, MIT Press, 1986.
- [18] A. Shashua, "Geometry and Photometry in 3D Visual Recognition", PhD thesis, MIT, 1992.
- [19] Radiance Synthetic Imageing System <http://radsite.lbl.gov/radiance/HOME.html>